

Phase separations in a copolymer–copolymer mixture

This article has been downloaded from IOPscience. Please scroll down to see the full text article.

2006 J. Phys.: Condens. Matter 18 837

(<http://iopscience.iop.org/0953-8984/18/3/006>)

View [the table of contents for this issue](#), or go to the [journal homepage](#) for more

Download details:

IP Address: 129.252.86.83

The article was downloaded on 28/05/2010 at 08:49

Please note that [terms and conditions apply](#).

Phase separations in a copolymer–copolymer mixture

Jin-Jun Zhang^{1,2}, Guojun Jin^{1,3} and Yuqiang Ma¹

¹ National Laboratory of Solid State Microstructures and Department of Physics, Nanjing University, Nanjing 210093, People's Republic of China

² Department of Physics, Shanxi Normal University, Linfen 041004, People's Republic of China

E-mail: gjin@nju.edu.cn

Received 7 July 2005, in final form 28 November 2005

Published 21 December 2005

Online at stacks.iop.org/JPhysCM/18/837

Abstract

We propose a three-order-parameter model to study the phase separations in a diblock copolymer–diblock copolymer mixture. The cell dynamical simulations provide rich information about the phase evolution and structural formation, especially the appearance of onion-rings. The parametric dependence and physical reason for the domain growth of onion-rings are discussed.

1. Introduction

The phase-ordering dynamics in soft matter systems has attracted much attention in the past two decades [1–7]. The microphase separation in block copolymers has been a hot topic both experimentally and theoretically [8–18]. These studies facilitate the development of new materials to achieve special properties. In the theoretical study of the general copolymer–homopolymer mixtures, Hong and Noolandi suggested that after a macrophase separation there would be a microphase separation in the copolymer-rich domain [8]. This prediction was verified experimentally by Koizumi, Hasegawa, and Hashimoto in binary mixtures of polystyrene–block–polyisoprene and homopolystyrene [10].

In recent years, field-theoretical approaches have been developed rapidly and adopted extensively in the study of polymer materials by using component densities as variables. A systematic acquaintanceship can be acquired in several excellent review articles [19–21]. Among various possible schemes based on mean-field approximations, the self-consistent field theory [22, 23] and dynamic density functional theory [24, 25] are best known. They can be used to obtain relatively detailed information of polymer mixtures, especially the static conformation and phase diagrams of mixtures. On the other hand, the time-dependent Ginzburg–Landau theory [26, 27], using the truncated expansions in a more complicated free energy compared with the self-consistent field method and dynamic density functional method, has often been applied to describe the dynamic behaviour of phase separations, in the situation where the polymer–polymer interface tensions may be more dominant, while the details of polymeric

³ Author to whom any correspondence should be addressed.

chains can be ignored. In this way, much rich novel structure was discovered by Ohta and Ito in their study on the phase separation in copolymer–homopolymer mixtures [9]. We have also reported numerically the structural formation in this kind of binary mixtures by containing mobile particles with a preferential interaction to one component [4].

It is interesting to note that so far less research has been done on the phase separation of copolymer–copolymer mixtures, whether experimentally or theoretically. However, with the development of industrial synthesis technology, it is more common that two different copolymers could be mixed. Therefore, the study of the dynamics of phase separations is obviously important for the mixtures composed of two different copolymers. In this paper, we investigate the phase separation in a copolymer–copolymer mixture, and obtain rich domains in this mixture. The other parts of this paper is organized as follows. Section 2 is devoted to the description of the model and method. In section 3 the numerical results and discussions are presented. Finally, a brief conclusion is given in section 4.

2. Model and method

We consider on a substrate surface there is a phase-separating film consisting of two different diblock copolymers. Each copolymer chain of one diblock copolymer is composed of A and B monomers with a short-range repulsive interaction between them, whereas that of the other diblock copolymer is composed of C and D monomers, and the interaction between C and D monomers is also short-range repulsive. The B monomers and D monomers in two different copolymers are mutually incompatible with each other. The interaction between the mixture and the substrate surface is assumed to be negligible, i.e., the substrate is neutral to the polymer blend. In addition, the hydrodynamic effects, for simplicity, are ignored in the present model. The coordinates of the planar surface are defined in the x and y directions.

For describing the system, several parameters are defined. N_A , N_B , N_C , and N_D are the polymerization indices of blocks A, B, C, and D, respectively. In the case of symmetric diblock copolymers which is considered here, the polymerization indices of the A and B blocks are equal, that is also true for the C and D blocks. We use χ_{ij} denote the interaction between monomers i and j , where $i, j = A, B, C$, and D. In the process of phase separations, fluctuations are dominant, so we should investigate the local volume fractions of monomers A, B, C, and D. They are denoted, respectively, by $\phi_A(x, y)$, $\phi_B(x, y)$, $\phi_C(x, y)$, and $\phi_D(x, y)$. Under the incompressibility condition, that is the total density $\phi_A(x, y) + \phi_B(x, y) + \phi_C(x, y) + \phi_D(x, y)$ is constant, three of the local volume fractions are independent. Therefore it is reasonable to take $\psi(x, y) = \phi_A(x, y) + \phi_B(x, y)$, $\phi(x, y) = \phi_A(x, y) - \phi_B(x, y)$, and $\xi(x, y) = \phi_C(x, y) - \phi_D(x, y)$ as the independent variables. These three quantities can be taken as the order parameters to describe the phase behaviour of the system. Among them $\psi(x, y)$ reflects the segregation of two different copolymers, whereas $\phi(x, y)$ and $\xi(x, y)$ give the local concentration differences between monomers A and B and between monomers C and D, respectively.

It is natural here to propose a three-order-parameter model, developed from the previous two-order-parameter model [9, 26, 27], in which the free-energy functional of the system is given by

$$F = F_L + F_S. \quad (1)$$

The long-range part F_L is given by

$$F_L = \frac{\alpha}{2} \int \int d\mathbf{r} d\mathbf{r}' G_1(\mathbf{r}, \mathbf{r}') [\phi(\mathbf{r}) - \phi_0][\phi(\mathbf{r}') - \phi_0] + \frac{\beta}{2} \int \int d\mathbf{r} d\mathbf{r}' G_2(\mathbf{r}, \mathbf{r}') [\xi(\mathbf{r}) - \xi_0][\xi(\mathbf{r}') - \xi_0], \quad (2)$$

where α and β are positive constants. $G_1(\mathbf{r}, \mathbf{r}')$ and $G_2(\mathbf{r}, \mathbf{r}')$ are the Green functions defined by the equations $-\nabla^2 G_1(\mathbf{r}, \mathbf{r}') = \delta_1(\mathbf{r} - \mathbf{r}')$ and $-\nabla^2 G_2(\mathbf{r}, \mathbf{r}') = \delta_2(\mathbf{r} - \mathbf{r}')$, while ϕ_0 and ξ_0 are the spatial averages of ϕ and ξ , respectively. We should set $\phi_0 = 0$ and $\xi_0 = 0$ in the case of symmetric copolymers. In contrast to the long-range part, the short-range part F_S is a little more complicated and is given by

$$F_S = \int \int dx dy \left[\frac{d_1}{2} (\nabla \psi)^2 + \frac{d_2}{2} (\nabla \phi)^2 + \frac{d_3}{2} (\nabla \xi)^2 + f(\psi, \phi, \xi) \right], \quad (3)$$

where the d_1 , d_2 , and d_3 terms correspond to the surface tensions. The local interaction term $f(\psi, \phi, \xi)$ could be replaced by $f(\eta, \phi, \xi)$, where $\eta = \psi - \psi_c$ [9] with ψ_c being the volume fraction at the critical point of the macrophase separation of two different copolymers.

It is obvious that the important physical results will be mainly included in the local interaction term $f(\eta, \phi, \xi)$. For further treatment, we can take its form in a phenomenological approach [9] as

$$f(\eta, \phi, \xi) = v_1(\eta) + v_2(\phi) + v_3(\xi) + b_1 \eta \phi - b_{11} \eta \xi - \frac{1}{2} b_2 \eta \phi^2 + \frac{1}{2} b_{22} \eta \xi^2, \quad (4)$$

where the functions $v_1(\eta)$, $v_2(\phi)$, and $v_3(\xi)$ are assumed to be even with respect to the arguments. For two symmetric diblock copolymers, the $\eta^2 \phi$ term and the $\eta^2 \xi$ term will vanish, so they merge in our model. In fact, we can obtain $f(\eta, \phi, \xi)$ from the Flory–Huggins free energy [28] for our four-monomer mixture as

$$f(\{\phi_i\}) = \sum_i \frac{1}{N_i} \phi_i \ln \phi_i + \sum_{ij} \chi_{ij} \phi_i \phi_j, \quad (5)$$

with $i, j = A, B, C, D$. According to the definitions of the three order parameters, the local volume fractions ϕ_A , ϕ_B , ϕ_C , and ϕ_D can be replaced by η , ϕ , and ξ . Then by expanding equation (5) in terms of the parameters η , ϕ , and ξ , we regain equation (4) in which $v_1(\eta) = -\frac{1}{2} c_1 \eta^2 + \frac{1}{4} \mu_1 \eta^4$ as well as for $v_2(\phi)$ and $v_3(\xi)$. All the coefficients c_s , μ_s , and b_s are determined, for example, $b_1 = (-\chi_{AC} - \chi_{AD} + \chi_{BC} + \chi_{BD})/4$, $b_{11} = (-\chi_{AC} + \chi_{AD} - \chi_{BC} + \chi_{BD})/4$, and $b_2 = b_{22} = (N_A^{-1/2} + N_C^{-1/2})^2/2$ for $N_A = N_B$ and $N_C = N_D$ in the symmetric case. In addition, the critical composition is also obtained as $\psi_c = N_C^{1/2}/(N_C^{1/2} + N_A^{1/2})$. Without losing generality, we take b_1 and b_2 as positive constants just like b_2 and b_{22} . The requirements for $b_1 > 0$ and $b_2 > 0$ could be satisfied by adopting a relatively large repulsive interaction between monomers B and D. It is now clear that the b_1 term and b_{11} term originate from the short-range interactive between monomers, whereas the b_2 term and b_{22} term arise from the conformation entropy of the copolymers. Equation (4) prescribes the minimal model of the short-range part of the free energy in our system. From the b_2 term and b_{22} term, one can see that a microphase separation could occur in the copolymers. In fact, the b_2 term implies that a large absolute value of $\phi(x, y)$ is favourable in the region $\eta(x, y) > 0$, whereas the b_{22} term means that a large absolute value of $\xi(x, y)$ is more favourable in the region $\eta(x, y) < 0$. Competitive interactions in the free-energy functional will lead to phase separations in our copolymer–copolymer mixture.

In terms of the free energy functional in equations (1)–(4), we can establish a set of three coupled equations for the three order parameters; they are

$$\frac{\partial \eta}{\partial t} = M_\eta \nabla^2 \frac{\delta F}{\delta \eta}, \quad (6)$$

$$\frac{\partial \phi}{\partial t} = M_\phi \nabla^2 \frac{\delta F}{\delta \phi}, \quad (7)$$

$$\frac{\partial \xi}{\partial t} = M_\xi \nabla^2 \frac{\delta F}{\delta \xi}, \quad (8)$$

where M_η , M_ϕ , and M_ξ are the positive transport coefficients.

The numerical solutions of the above model system can be carried out in an $L \times L$ two-dimensional square lattice under the periodic boundary conditions, by using the approach of cell dynamical simulation (CDS) proposed by Oono and Puri [29, 30]. The CDS equations corresponding to equations (6)–(8), in their space-time discretized forms, are written as follows:

$$\eta(x, y, t + \Delta t) = \eta(x, y, t) + M_\eta(\langle\langle I_\eta \rangle\rangle - I_\eta), \quad (9)$$

$$\phi(x, y, t + \Delta t) = \phi(x, y, t) + M_\phi\{\langle\langle I_\phi \rangle\rangle - I_\phi\} - \alpha[\phi(x, y, t) - \phi_0], \quad (10)$$

$$\xi(x, y, t + \Delta t) = \xi(x, y, t) + M_\xi\{\langle\langle I_\xi \rangle\rangle - I_\xi\} - \beta[\xi(x, y, t) - \xi_0], \quad (11)$$

where

$$I_\eta = -d_1(\langle\langle \eta \rangle\rangle - \eta) - A_\eta \tanh \eta + \eta + b_1\phi - b_{11}\xi - \frac{1}{2}b_2\phi^2 + \frac{1}{2}b_{22}\xi^2, \quad (12)$$

$$I_\phi = -d_2(\langle\langle \phi \rangle\rangle - \phi) - A_\phi \tanh \phi + \phi + b_1\eta - b_2\eta\phi, \quad (13)$$

$$I_\xi = -d_3(\langle\langle \xi \rangle\rangle - \xi) - A_\xi \tanh \xi + \xi - b_{11}\eta + b_{22}\eta\xi. \quad (14)$$

In equations (12)–(14), there are three similar terms $-A_\eta \tanh \eta + \eta$, $-A_\phi \tanh \phi + \phi$, and $-A_\rho \tanh \rho + \rho$. They are good approximations for the derivatives $dv_1(\eta)/d\eta$, $dv_2(\phi)/d\phi$, and $dv_3(\rho)/d\rho$ according to the CDS method. These derivatives are the odd functions of their order parameters corresponding to the even functions of the local free-energy densities $v_1(\eta)$, $v_2(\phi)$, and $v_3(\rho)$. It is understood that coefficients A_η , A_ϕ , and A_ξ describe the local free-energy densities. In general, they are larger than one [30]. An average for a variable Q used in equations (9)–(14) is defined by

$$\langle\langle Q \rangle\rangle = \frac{1}{6} \sum_{\text{NN}} Q + \frac{1}{12} \sum_{\text{NNN}} Q, \quad (15)$$

where the subscripts NN and NNN stand for the nearest-neighbour and next-nearest-neighbour cells, respectively.

Our simulations of the model system are performed by choosing the parameters with $L = 128$, $A_\eta = 1.3$, $A_\phi = 1.1$, $A_\xi = 1.1$, $d_1 = 1.0$, $d_2 = 0.5$, $d_3 = 0.5$, and $M_\eta = M_\phi = M_\rho = 1$, according to the previous work. For the original cell dynamics system, the lattice size (Δx or Δy) and the time step (Δt) are both set to be unity.

3. Numerical results and discussions

For a two-dimensional diblock copolymer–diblock copolymer mixture, one can study its phase behaviour by suitably choosing the free parameters and using the CDS equations (9)–(14). Beginning from a homogeneous distribution of monomers A, B, C, and D, the system will evolve into a state of phase separations. It is interesting to point out that the homogeneous distribution does not represent the equilibrium state of the system. In fact, the free energy, especially its short-range part, provides a kind of chemical potential as well as the surface tensions to drive the system from an unstable state to the stable state which characterizes phase separations. However, it is necessary to take into account some numerical errors as perturbations in the system to facilitate the transformation from the initial non-equilibrium homogeneous state to an equilibrium inhomogeneous state. In our calculation, a random distribution of very small fluctuations is imposed onto the initial state, then, as the system is evolving, phase separations can take place. The process of phase separations includes macrophase separation and microphase separation. In fact, macrophase and microphase evolve almost sequentially. Following the macrodomain growth, the microdomain structures become complex. In particular, the onion-ring structure can appear in the system. For clearness, we denote the A-rich domain for $\phi > 0$ and the B-rich domain for $\phi < 0$, respectively, by the

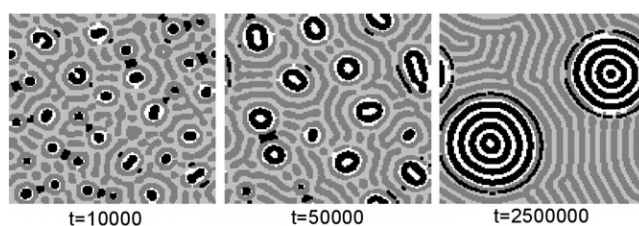


Figure 1. Pattern evolution of a two-dimensional lattice for $\alpha = 0.04$, $\beta = 0.03$, $b_1 = 0.081$, $b_{11} = 0.1$, $b_2 = b_{22} = 0.2$, and $\bar{\eta} = 0.3$. Phase A is represented by the grey region, phase B by the light grey region, phase C by the black region, and phase D by the white region.

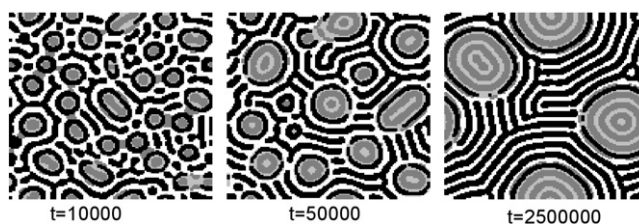


Figure 2. Pattern evolution of a two-dimensional lattice for $\bar{\eta} = -0.3$ while the other parameters are the same as in figure 1. Phase A is represented by the grey region, phase B by the light grey region, phase C by the black region, and phase D by the white region.

grey and light grey, whereas the C-rich domain for $\xi > 0$ and the D-rich domain for $\xi < 0$ by the black and white colours, respectively.

An evolution process in formation of an onion-ring structure is displayed in figure 1 for $\alpha = 0.04$, $\beta = 0.03$, $b_1 = 0.081$, $b_{11} = 0.1$, $b_2 = b_{22} = 0.2$, and $\bar{\eta} = 0.3$, at times corresponding to $t = 10\,000$, $50\,000$, $2\,500\,000$, respectively. From figure 1, it is seen that at $t = 10\,000$ the phase separation is not obvious. In the evolution process, the macrophase separation occurs first. With the macrophase separation proceeding the microphase separation also emerges, as shown at $t = 50\,000$ in figure 1. With the time step increased further, for example at $t = 2\,500\,000$, the pretty onion-ring structure appears in the C–D copolymer, which coexists with the bicontinuous striped structure in the A–B copolymer. It is found that the grey and black colours aggregate at the interface between the two kinds of copolymers, because phase A and phase C are compatible with each other. From the formation of onion-rings, it can be seen that this structure is the result of the competition between the b_{22} term and the b_{11} term as well as the b_1 term. From our simulations, beautiful onion-ring structure is obtained by adjusting b_1 when b_{11} and b_{22} are fixed.

In order to investigate the effect from the relative concentrations of the two copolymers, we change only the initial composition ratio of A–B copolymer and C–D copolymer. In comparison with figure 1, figure 2 displays the evolution patterns for $\bar{\eta} = -0.3$ while the other parameters are the same as in figure 1. From figure 2, it is easy to see that the evolution patterns are roughly the reverse of those corresponding to figure 1. Now the C–D copolymer is the dominant phase, in which the onion-rings are formed in the A–B copolymer.

To understand the onion-ring structure further, we examine in detail the dependence of its stable structure on the phenomenological parameters b_{11} , which is determined by the interactions between monomers in the copolymers. Figure 3 displays the patterns at $t = 2\,500\,000$ with variation of the parameter b_{11} from 0.02 to 0.06. As $b_{11} = 0.02$, the striped microdomains in the C–D copolymer are basically perpendicular to the macrodomain

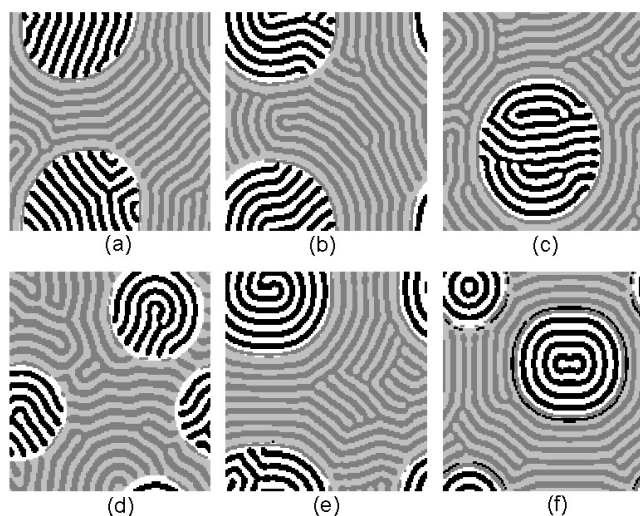


Figure 3. Patterns on a two-dimensional lattice for $\alpha = \beta = 0.03$, $b_1 = 0.065$, $b_2 = b_{22} = 0.2$, and $\bar{\eta} = 0.3$. (a) $b_{11} = 0.02$, (b) $b_{11} = 0.024$, (c) $b_{11} = 0.04$, (d) $b_{11} = 0.044$, (e) $b_{11} = 0.047$, and (f) $b_{11} = 0.06$. Phase A is represented by the grey region, phase B by the light grey region, phase C by the black region, and phase D by the white region.

interfaces, and the microdomain curvature in the C–D copolymer is small, as in figure 3(a). With increasing b_{11} , the stripes in the C–D copolymer start to bend, resulting in the striped microdomains changing from almost perpendicular to partly parallel to the interfaces, as shown in figure 3(b). As b_{11} increases again, the parallel part extends whereas the perpendicular part decreases gradually, as shown in figures 3(c) and (d). Continuously increasing b_{11} , almost all of the striped microdomains become parallel to the macrodomain interfaces, and the pretty onion-rings emerge in the C–D copolymer, as displayed in figures 3(e) and (f). From figure 3(f) it can be seen that the striped microdomains are perfectly parallel to the macrodomain interface, consequently realizing the transition of the striped microdomain structure from perpendicular to parallel to the macrodomain interfaces.

From figures 3(a) to (f), it is found that the striped microdomains in the A–B copolymer are parallel to the macrodomain interfaces at all times, and their structure does not change on the whole. The process can be understood as follows: on one hand, the striped microdomain structure in the A–B copolymer does not vary, because the effect of b_{11} on the A–B copolymer is very weak. On the other hand, the striped microdomains in the C–D copolymer transit from the perpendicular to parallel to the macrodomain interfaces with increasing b_{11} . The parameter b_{11} represents the strength of the repulsive interaction of the A–B copolymer to the D phase in the C–D copolymer. When b_{11} is small, the D phase is weakly affected by the A–B copolymer, so the C phase and D phase can all aggregate in the macrodomain interfaces, resulting the striped microdomains perpendicular to the macrodomain interfaces. As b_{11} increases, the strength with which the D phase is acted on by the A–B copolymer also increases, and it makes the D phase not favourable in the macrodomain interfaces, thereby the D phase at the macrodomain interfaces diminishes, and the striped microdomains change from perfectly perpendicular to partly parallel to the macrodomain interfaces. Finally, the interface of macrophase separation is dominated perfectly by the C phase, resulting in the ring-like patterns.

In order to study the domain growth, we would calculate numerically the domain size $R(t)$ as a function of time. The domain size $R(t)$ can be derived from the inverse of the first

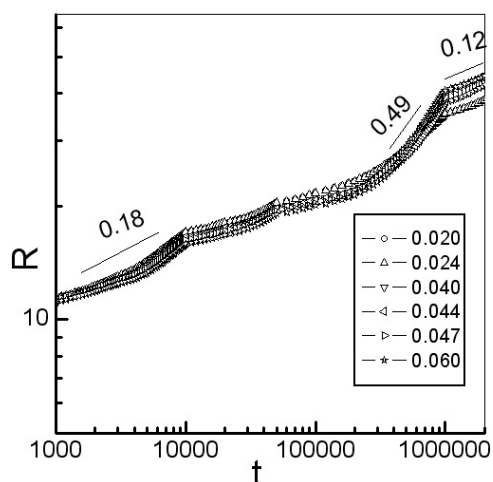


Figure 4. Time evolution of the macrodomain size as a characteristic length for figure 3.

moment of the structure factor $S(\mathbf{k}, t)$ as

$$R(t) = 2\pi/\langle k(t) \rangle, \quad (16)$$

where

$$\langle k(t) \rangle = \int d\mathbf{k} k S(\mathbf{k}, t) / \int d\mathbf{k} S(\mathbf{k}, t). \quad (17)$$

In fact, the structure factor $S(\mathbf{k}, t)$ is determined by the Fourier component of the spatial concentration distribution [30]. The results are averaged over five independent runs.

Figure 4 shows the time evolution of the macrodomain size $R(t)$ as a function of time in the double-logarithmic plots; the curves correspond to the various cases in figure 3, respectively. From figure 4, it is seen that as b_{11} changes from 0.02 to 0.06, the growth processes of the macrodomain are almost invariant, only at the latest stage of time evolution is there a little difference in the macrodomain size. This indicates that the interactions between the monomers hardly influence the growth of macrodomains of onion-rings. In fact, the b_{11} term mainly determines the morphology at the interfaces of macrodomains of onion-rings. From the growth exponent in figure 4, it can be seen that the macrodomains of onion-rings grow slowly in the early stage, but rapidly in the middle stage, especially in the stage from $t = 200\,000$ to $t = 1\,000\,000$. In the later stage, the growth speed of macrodomains decreases again. From figure 4 it can also be seen that with the value of b_{11} changing, the macrodomains of onion-rings almost grow by the same growth exponent in the latest stage.

4. Conclusion

Based on the three-order-parameter model, we have studied the phase separations in a diblock copolymer–diblock copolymer mixture. It has been found by the cell dynamics simulations that the onion-ring structure for one copolymer would appear in the background of the other copolymer. Macroscopically, from the local free-energy density, there is no doubt that the beneficial condition for onion-rings is the strong repulsive interaction between the sum and difference of one copolymer itself, as well as the attractive interaction between the sum of one copolymer and the difference of the other copolymer; furthermore, microscopically, one

strong local interaction between two kinds of monomers from two different copolymers is necessary for the formation of onion-rings. It is expected that the efficient values of these interactions between monomers are also related to the other parameters of the system. It has been experimentally verified previously that the onion-ring structure occurs in a homopolymer–copolymer mixture [10]. We can expect this structure would also emerge in a copolymer–copolymer mixture. We have examined in detail the formation process and domain growth of the onion-ring structure, and obtained various onion-rings by choosing suitable phenomenological parameters, which are determined by the interactions between monomers and the polymerization indices of copolymers.

It is worth mentioning that we have mainly concerned with the ordering and phase separations in copolymer–copolymer mixtures. Our present simulations are based on the time-dependent Ginzburg–Landau theory, with closely related cell dynamical simulations, which is suitable to study the dynamical process of the system and save time of computations. This phenomenological approach, as is concise and universal, can successfully describe the time evolution in macrophase separation as well as microphase separation. However, it is limited in describing morphological minutiae. If the structural details must be considered, and the equilibrium properties are much more concerned with, we should take advantage of more powerful field-theoretical methods, such as the self-consistent field theory or dynamic density functional theory. The present model and simulations provide beneficial suggestions for experimentally realizing onion-ring structure on phase-separation films consisting of diblock copolymer–diblock copolymer mixtures.

Acknowledgments

This work was supported by the National Natural Science Foundation of China under grants Nos 10334020, 1002100, 20490221, 10574061 and 60371013 and the Provincial Natural Science Foundation of Jiangsu under grant No BK2002086.

References

- [1] Roland C and Grant M 1988 *Phys. Rev. Lett.* **60** 2657
- [2] Taniguchi T and Onuki A 1996 *Phys. Rev. Lett.* **77** 4910
- [3] Gonnella G, Orlandini E and Yeomans J M 1997 *Phys. Rev. Lett.* **78** 1695
Gonnella G, Orlandini E and Yeomans J M 1998 *Phys. Rev. E* **58** 480
- [4] Ma Y Q 2000 *Phys. Rev. E* **62** 8207
Tang Y L and Ma Y Q 2002 *J. Chem. Phys.* **116** 7719
Zhu Y J and Ma Y Q 2002 *J. Chem. Phys.* **117** 10207
Zhang J J, Jin G and Ma Y Q 2005 *Phys. Rev. E* **71** 051803
Zhang J J, Jin G and Ma Y Q 2005 *Eur. Phys. J. E* **18** 359
- [5] Sabra M C, Gilhoj H and Mouritsen O G 1998 *Phys. Rev. E* **58** 3547
- [6] Keblinski P, Kumar S K, Maritan A, Koplik J and Banavar J 1996 *Phys. Rev. Lett.* **76** 1106
- [7] Corberi F, Gonnella G and Lammura A 1999 *Phys. Rev. Lett.* **83** 4057
- [8] Hong K M and Noolandi J 1983 *Macromolecules* **16** 1083
- [9] Ohta T and Ito A 1995 *Phys. Rev. E* **52** 5250
- [10] Koizumi S, Hasegawa H and Hashimoto T 1994 *Macromolecules* **27** 6532
- [11] Ohta T and Kawasaki K 1986 *Macromolecules* **19** 2621
- [12] Kawasaki K, Ohta T and Kohrogui M 1988 *Macromolecules* **21** 2972
- [13] Chen H and Chakrabarti A 1998 *J. Chem. Phys.* **108** 6897
- [14] Chen Z R, Kornfield J A, Smith S D, Grothaus J T and Satkowski M M 1997 *Science* **277** 1248
- [15] Thurn-Albrecht T, Schotter J, Kästle G A, Emley N, Shibauchi T, Krusin-Elbaum L, Guarini K, Black C T, Tuominen M T and Russell T P 2000 *Science* **290** 2126
- [16] Kim S O, Solak H H, Stoykovich H, Ferrie N J, de Pablo J J and Nealey P F 2003 *Nature* **424** 441

-
- [17] Jeong U, Ryu D Y, Kho D H, Kim J K, Goldbach J T, Kim D H and Russell T P 2004 *Adv. Mater.* **16** 533
- [18] Qi S and Wang Z G 1997 *Phys. Rev. E* **55** 1682
- [19] Glotzer S C and Paul W 2002 *Annu. Rev. Mater. Res.* **32** 401
- [20] Fredrickson G H, Ganesan V and Drolet F 2002 *Macromolecules* **35** 16
- [21] Müller M and Schmid F 2005 *Adv. Polym. Sci.* **185** 1
- [22] Matsen M W 1997 *J. Chem. Phys.* **106** 7781
Matsen M W 1997 *J. Chem. Phys.* **107** 8110
- [23] Reister E, Muller M and Binder K 2001 *Phys. Rev. E* **64** 041804
Muller M 2002 *Phys. Rev. E* **65** 030802
- [24] Fraaije J G E M, van Vlimmeren B A C, Maurits N M, Postma M, Evers O A, Hoffmann C, Altevogt P and Goldbeck-Wood G 1997 *J. Chem. Phys.* **106** 4260
Maurits N M and Fraaije J G E M 1997 *J. Chem. Phys.* **107** 5879
- [25] Morita H, Kawakatsu T and Doi M 2001 *Macromolecules* **34** 8777
Morita H, Kawakatsu T, Doi M, Yamaguchi D, Takenaka M and Hashimoto T 2002 *Macromolecules* **35** 7473
- [26] Komura S and Kodama H 1997 *Phys. Rev. E* **55** 1722
- [27] Roan J and Shakhnovich E I 1999 *Phys. Rev. E* **59** 2109
- [28] Huang C, Olvera de la Cruz M and Swift B W 1995 *Macromolecules* **28** 7996
- [29] Oono Y and Puri S 1987 *Phys. Rev. Lett.* **58** 836
Puri S and Oono Y 1988 *Phys. Rev. A* **38** 1542
- [30] Oono Y and Puri S 1987 *Phys. Rev. A* **38** 434
Shinozaki A and Oono Y 1992 *Phys. Rev. A* **45** 2126
Shinozaki A and Oono Y 1993 *Phys. Rev. E* **48** 2622